journal

J. Am. Ceram. Soc., 78 [6] 1431–38 (1995)

Contact Fatigue of a Silicon Carbide with a Heterogeneous Grain Structure

Nitin P. Padture*,† and Brian R. Lawn*

Materials Science and Engineering Laboratory, National Institute of Standards and Technology, Gaithersburg, Maryland, 20899

A comparative study of cyclic fatigue damage from Hertzian contacts in silicon carbide ceramics with *homogeneous* microstructure (fine, equiaxed grains, strong grain boundaries) and *heterogeneous* microstructure (coarse, contiguous elongate grains, weak interphase boundaries) is presented. Observations of the surface and subsurface damage patterns using optical microscopy reveal fundamentally different cyclic fatigue mechanisns: in the homogeneous material, by slow growth of a well-developed cone crack outside the contact area; in the heterogeneous material, by progressive mechanical degradation within a distributed damage zone below the contact area. Scanning electron micrographs of the latter material show copious fine debris in the damage zone, consistent with a degradation mechanism by frictional attrition by forward–reverse sliding at the weak interphase boundaries. Acoustic emission is recorded during both load and unload half-cycles, confirming hysteresis in the sliding process. Flexure tests indicate initially slight strength losses from the cyclic contact damage in both microstructures, followed by accelerated losses at higher numbers of cycles. The underlying basis for establishing an analytical model of damage accumulation in the heterogeneous microstructure in terms of shear-fault sliding, and for designing microstructures for optimal properties in fatigue and wear applications, is foreshadowed.

I. Introduction

In RECENT studies it has been demonstrated that the mechanical properties of silicon carbide can be profoundly influenced by developing a heterogeneous microstructure featuring contiguous platelets with residual weak interphase boundaries.[1–3] Relative to a homogeneous silicon carbide with equiaxed microstructure and strong grain boundaries, the new heterogeneous material showed a markedly reduced sensitivity to the starting size of Vickers indentation flaws,[1,2] i.e., an enhanced "flaw tolerance." Such flaw tolerance indicates a rising toughness curve, with enhanced toughness in the long-crack domain due to crack-interface, grain-interlock bridging.[4–7] Conversely, the toughness in the short-crack domain is diminished, due to local residual tensile stresses at the weak interphase boundaries.[6,7] Since the selection of silicon carbide ceramics for such structural components as bearings, rotors, valves, and nozzles is more likely to depend on short-crack properties, particularly in the context of strength and wear, it is evident that conventional long-crack testing procedures may not always be reliable sources of design data.

One way of obtaining data in the short-crack domain is by the Hertzian contact test.[3,8–11] In the simplest form of this test, a hard sphere is brought into contact with a polished specimen surface in single-cycle loading, and the ensuing damage is analyzed by microscopy and other means. The "blunt" spherical indenter geometry is characterized by a zero normal pressure at initial contact,[12] so the onset and evolution of irreversible damage with increasing load may be studied as one traverses an "indentation stress–strain curve."[8,10,13] The nature of the irreversible damage depends strongly on the ceramic microstructure: in finer, homogeneous ceramics it takes the form of classical cone fracture in the region of modest tension outside the contact circle;[12,14,15] in coarser, heterogeneous ceramics it appears as discrete microstructural-scale shear faults distributed in the region of compression–shear below the contact circle. The role of heterogeneity in effecting this change in damage mode is twofold: first, cone fracture is suppressed by deflection of incipient surface ring cracks along weak interfaces away from tensile stress trajectories;[15] second, local shear-induced sliding is induced at these same weak interfaces in the subsurface compression zone. The change is accompanied by a distinctive flattening of the indentation stress–strain curve, suggestive of a quasi brittle–ductile transition.[3]

The issue arises as to the influence of such microstructural heterogeneity on the response of silicon carbide ceramics to repeat loading, i.e., cyclic fatigue. Generally, fatigue studies have been conducted on ceramics using conventional long-crack fatigue tests borrowed from the metals community.[16–19] However, in view of the above-mentioned tendency toward inverse relations between toughness properties at opposite crack size extremes, extrapolation of long-crack results to the critical short-crack domain is at issue. It is in this context that the Hertzian test is especially attractive—progressive damage accumulation within an otherwise uncracked microstructure may be systematically monitored as a function of number of contact cycles.[8,20,21]

Accordingly, in the present paper we present observations of contact fatigue damage in homogeneous and heterogeneous silicon carbide in cyclic Hertzian tests. Optical and scanning electron microscopy observations reveal a progressive buildup of damage, most dramatically in the heterogeneous material. Sliding at interphase boundaries between silicon carbide platelets and surrounding second phase is confirmed as a principal damage mechanism. Acoustic emission experiments confirm reverse sliding during each cycle, indicating that fatigue is due to frictional attrition. Flexure tests conducted on specimens subjected to cyclic contacts show degradation in strength to be relatively slight in the heterogeneous silicon carbide, although the degradation does accelerate at higher numbers of cycles. The basis for establishing a micromechanical model of contact fatigue in ceramics with contiguous platelet microstructures is outlined.

II. Experimental Procedure

Heterogeneous silicon carbide specimens were prepared as previously described.[1,2] The material was 97% dense, with a

G. Grathwohl—contributing editor

Manuscript No. 193476. Received June 20, 1994; approved August 30, 1994.
Supported by the U.S. Air Force Office of Scientific Research and NIST.
*Member, American Ceramic Society.
†Guest scientist on leave from Department of Materials Science and Engineering, Lehigh University, Bethlehem, PA 18015. Now with University of Connecticut, Storrs, CT 06269.

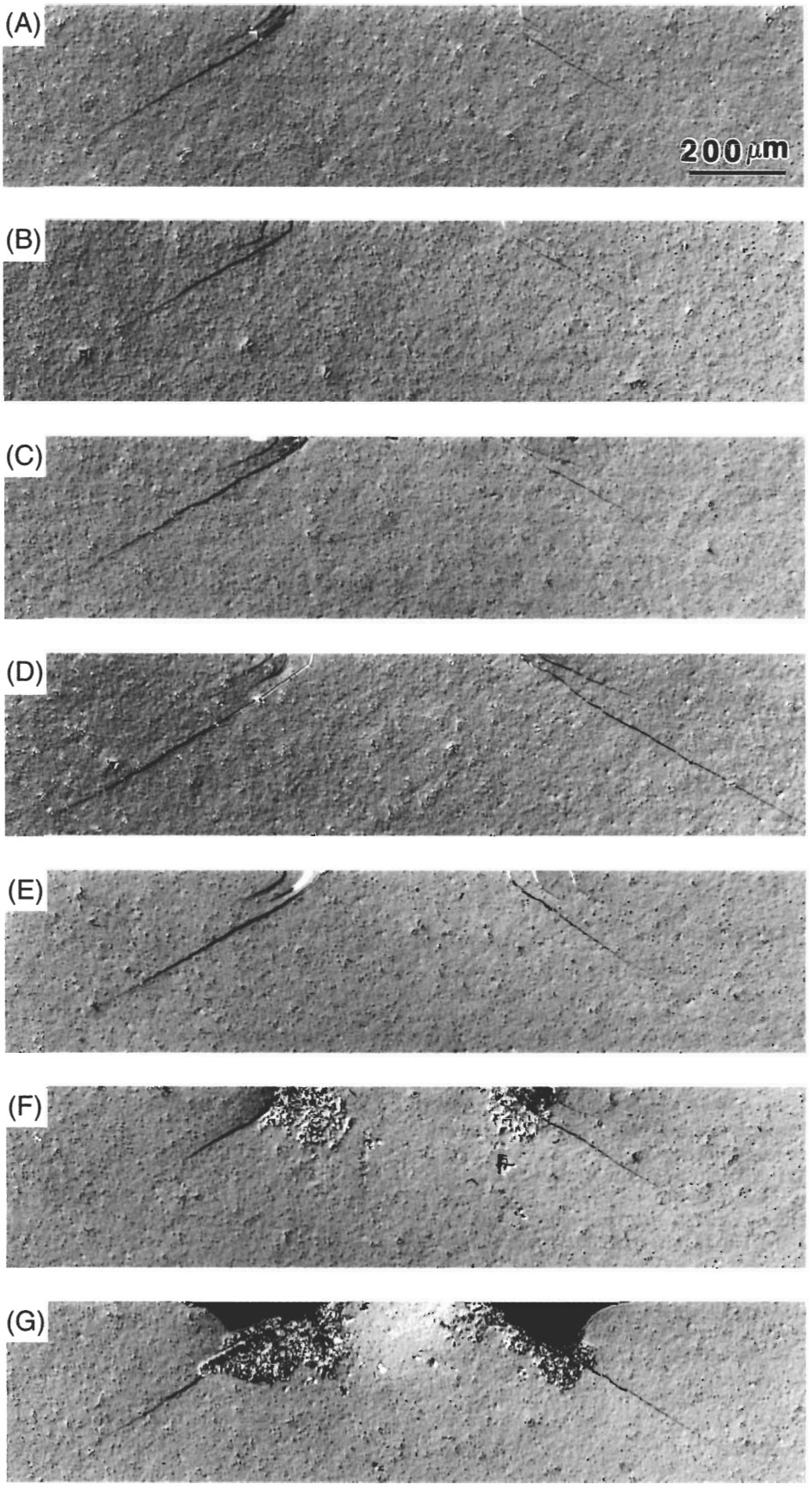

Fig. 1. Section views of Hertzian contact sites in homogeneous silicon carbide: number of cycles (A) $n = 1$, (B) $n = 10^1$, (C) $n = 10^2$, (D) $n = 10^3$, (E) $n = 10^4$, (F) $n = 10^5$, (G) $n = 10^6$. Indentations using a tungsten carbide sphere of radius 3.18 mm with sinusoidal cyclic load 0–1000 N at frequency 10 Hz, tests in air. Optical micrographs using Nomarski interference illumination. Note appearance of fine subsurface damage immediately below contact circle in (F) and detached collar in (G).

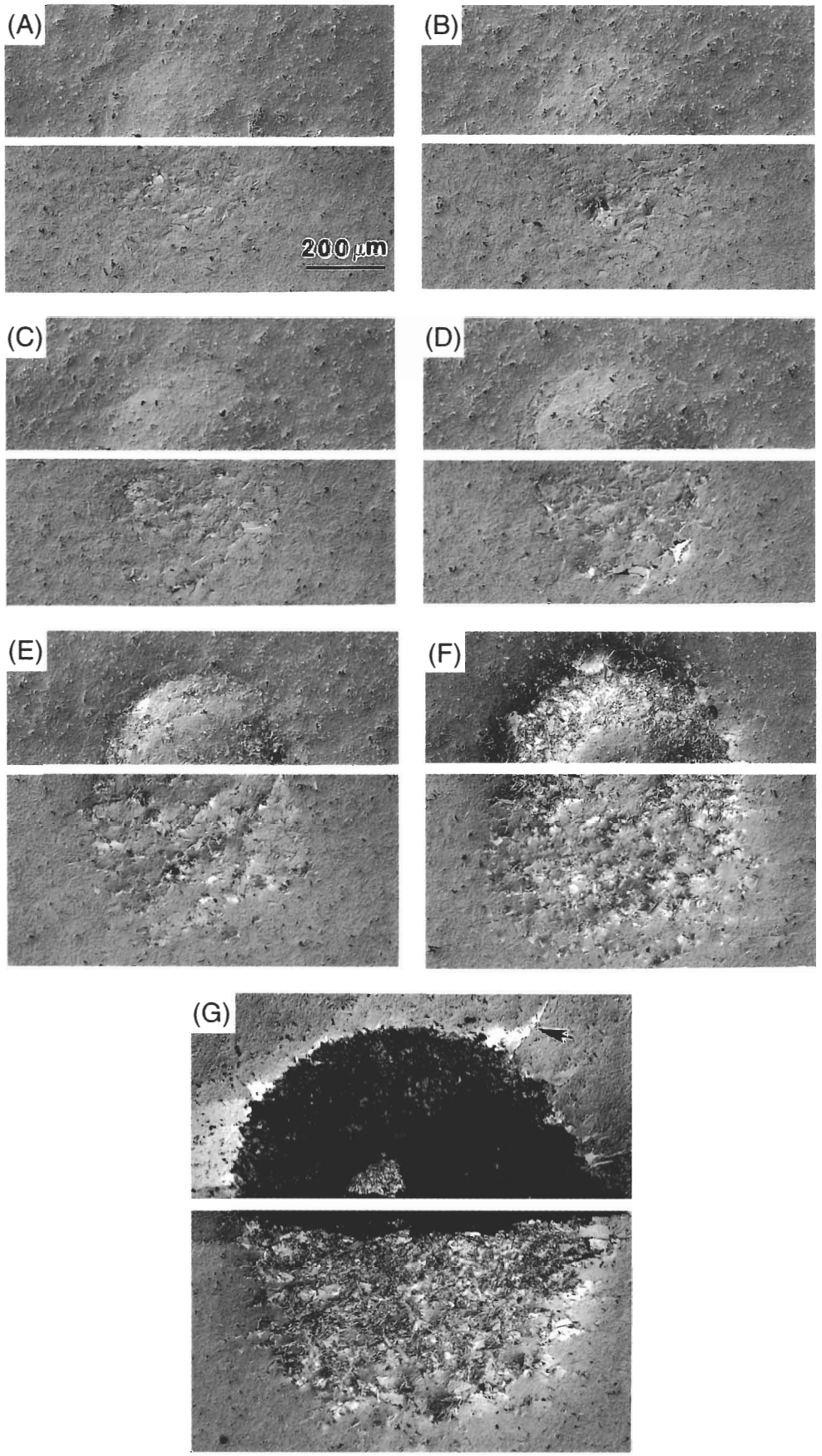

Fig. 2. Half-surface (upper) and section (lower) views of Hertzian contact sites in heterogeneous silicon carbide: number of cycles (A) $n = 1$, (B) $n = 10^1$, (C) $n = 10^2$, (D) $n = 10^3$, (E) $n = 10^4$, (F) $n = 10^5$, (G) $n = 10^6$. Indentations using tungsten carbide sphere of radius 3.18 mm with sinusoidal cyclic load 0–1000 N at frequency 10 Hz, tests in air. Optical micrographs using Nomarski interference illumination. Note progressive buildup of subsurface damage with increasing n, material removal and radial crack formation (arrow) in (G).

microstructure consisting of silicon carbide platelets ≈3 μm thick by ≈25 μm long, with 20 vol% yttrium aluminum garnet (YAG) grain boundary phase in the interstices. Fracture was intergranular,[1] with an interphase toughness ≈2 MPa·m$^{1/2}$.[2]

Homogeneous silicon carbide specimens for control testing were obtained ready fabricated from a commercial source (Hexoloy SA, Carborundum, Niagara Falls, NY). The material again was 97% dense, but with an equiaxed microstructure, grain size ≈4 μm. In this case the fracture was transgranular, indicating comparatively strong grain boundaries.

A special specimen configuration was used to obtain section as well as surface views of Hertzian contact damage in both the homogeneous and heterogeneous materials.[21] These specimens were prepared by bonding together two diamond polished (<1 μm surface finish) half-blocks 20 mm × 3 mm × 3 mm at a common interface with thin (<10 μm) cyanoacrylate-based adhesive (Loctite, Newington, CT). Subsequently, the top surfaces of the composite specimens were ground and diamond polished (<1 μm surface finish). Up to 10^6 repeat indentations were then made on the specimen surface symmetrically across the surface trace of the bonded interface with a tungsten carbide sphere of radius 3.18 mm using a servo-hydraulic universal testing machine (Model 8502, Instron, Canton, MA), with sinusoidal wave form at frequency 10 Hz. The peak load used for the microscopy studies was 1000 N, just above the onset of visible damage in both materials. This load corresponds to a contact pressure ≈6 GPa in silicon carbide, in the region of first deviation from linearity in the indentation stress–strain curve.[2] In most tests, the load was cycled between 0 and 1000 N, but in a select few instances the range was reduced to 400–1000 N after the first load half-cycle. All indentations were made under ambient conditions. The indented specimens were then separated by dissolving the adhesive in acetone. The top and side surfaces were gold coated and viewed optically in Nomarski illumination (Diphot, Nikon, Tokyo, Japan) and in a scanning electron microscope (Model 1830, Amray, Bedford, MA) to reveal the damage patterns.

Acoustic emission experiments (LOCAN 320, Physical Acoustics, Princeton, NJ) were performed to gain insight into the mechanisms of fatigue damage evolution during cyclic indentation. These experiments were made on bulk (unbonded) specimens 20 mm × 3 mm× 3 mm, again in air. Acoustic activity was recorded during load–unload–reload cycles using a piezoelectric transducer attached to the indentation surface with rubber cement. Data were recorded as accumulated signal energy versus elapsed time. To ensure sufficient signal intensity and time resolution, the loading conditions were changed relative to those used in the microscopy studies: namely, higher peak load 2000 N (but same minimum 400 N in partial unload experiments) with linear load–unload (sawtooth) ramps, and lower frequency 0.005 Hz.

For strength evaluation of the silicon carbide materials, disks 200 mm diameter and 2.5 mm thickness were ground and diamond polished on one face to 1 μm finish. Some disks were left unindented, for measurement of "laboratory" strengths. The others were indented over a load range 0–1000 N at the centers of the polished faces, each at a specific number of cycles, as described above for the microscopy studies. The disks were broken in biaxial flexure, indented sides in tension, using a three-point support and circular-flat loading fixture[22] on a universal testing machine (Model 1122, Instron, Canton, MA). A drop of dried silicone oil was placed on the indentation site immediately prior to the strength test, and flexure was applied rapidly (failure time <10 ms), to minimize environmental effects ("inert strength"). Strengths were calculated from the failure loads and specimen dimensions.[22] All broken disks were examined to confirm the source of failure: in the homogeneous silicon carbide, all breaks occurred from the cone cracks; in the heterogeneous silicon carbide some failures occurred from microstructural flaws, especially at lower numbers of contact cycles, in which case the data were included in the pool for laboratory strength.

III. Results

(1) Optical and SEM Observations

The first tests were run to determine the fatigue response of the homogeneous silicon carbide, as a baseline for comparison with the heterogeneous material. Figure 1 shows a sequence of section views of the contact damage from a row of indentations at increasing number of cycles n. A classical Hertzian crack[12,15] is observed at $n = 1$. The fracture is completely transgranular,[1,2] typical of low-toughness brittle solids. The crack forms outside the contact circle, where the contact stresses are tensile, and penetrates downward and outward into its ultimate cone geometry.[12,15,23] It is apparent from the sequence that the effect of n on the depth of the cone crack is insubstantial. One may conclude that the cone crack per se is not subject to fatigue, other than perhaps from minor effects of slow crack growth in this material[24] (Appendix). Some fatigue damage is evident outside the contact circle at high n, in the form of fine subsurface deformation buildup adjacent to the cone crack mouth in Fig. 1(F) and detached collar in Fig. 1(G), suggesting the existence of a secondary mechanical effect in the near-surface region.

By contrast, analogous runs in heterogeneous silicon carbide at the same loading conditions showed significant fatigue effects. Half-surface and section views of the contact damage buildup are included in Fig. 2. Instead of the traditional cone crack, distributed, discrete subsurface damage is apparent in the compression zone below the contact.[2] The deformation in this zone is driven by shear instead of tensile stresses.[8,10,12,25] The damage is barely perceptible at $n = 1$ (Fig. 2(A)), but expands in density and scale with increasing n until, at $n = 10^6$ (Fig. 2(G)), material begins to dislodge from the contact zone. At this point (and thereafter) macroscopic radial cracks begin to form (arrow in Fig. 2(G)).[12] We note the relative absence of damage in the contact center through Figs. 2(A) to 2(F), indicating suppression of the shear-driven deformation by the high compression stresses in this near-surface region.[9,10]

Figure 3 is another view of the damage in heterogeneous silicon carbide at $n = 10^6$, as in the preceding sequence, but with minimum load 400 N during the unload half-cycles. Relative to the corresponding view in Fig. 2(G) for zero minimum load, the damage is much reduced, indicating that a significant portion of the fatigue occurs at the lower load end of the unloading–reloading cycle. There is the suggestion of some

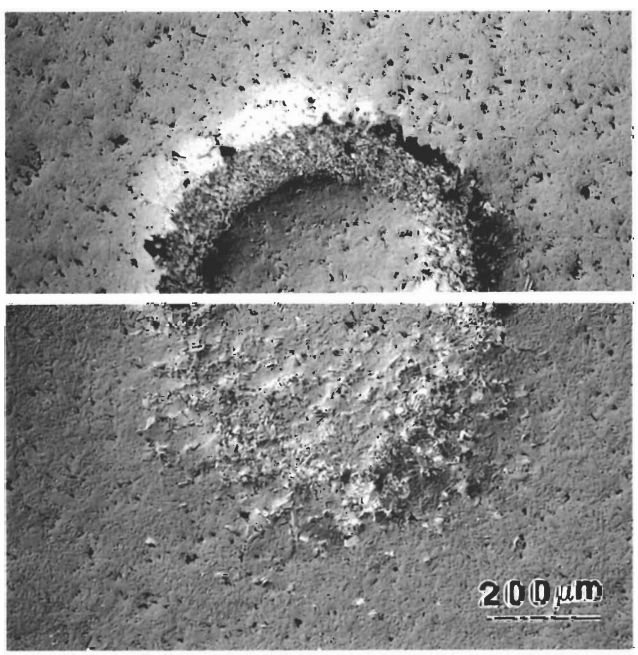

Fig. 3. Same as Fig. 2(G), but over reload–unload cyclic range 400–1000 N.

form of reversal in the damage process in this load region. We reinforce this suggestion in the next subsection.

High-magnification scanning electron micrographs of the subsurface damage zone at $n = 10^6$ in Fig. 2(G) are shown in Fig. 4. These micrographs reveal the microstructural discreteness of the cumulative damage process that constitutes the macroscopic deformation zone in the heterogeneous silicon carbide. Specifically, they provide evidence for sliding at the weak interfaces between silicon carbide platelets and YAG interstitial phase, in the form of frictional debris along the traces of the interphase boundaries and of associated voids left in the surface microstructure. No such debris was observed outside the damage zone in the cyclic tests, or indeed within the zone at low n. It is noteworthy that this debris remains attached after separation and cleaning of the bonded half-block specimens, indicative of strong electrostatic adhesion forces.[26,27] Energy-dispersive spectroscopy revealed the presence of Si, C, O, Al, and Y in the debris, confirming attrition of both the SiC and YAG phases.

(2) Acoustic Emission

Acoustic activity was monitored during cyclic loading during Hertzian indentation of silicon carbide specimens. Control tests on the homogeneous material simply showed large spike signals at each cone crack pop-in. No other emissions were recorded, either in the first or subsequent cycles.

Acoustic activity in the heterogeneous material was also discrete, but each signal was much smaller and the number of signals much greater. Results of selected runs are shown in Figs. 5–7, as plots of cumulative acoustic energy. The units in these diagrams are arbitrary, but the scale is the same in all cases. A plot of load versus elapsed time is included at the bottom of each diagram.

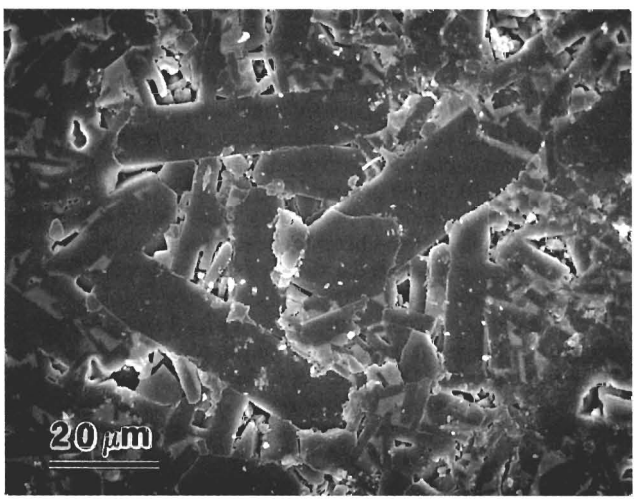

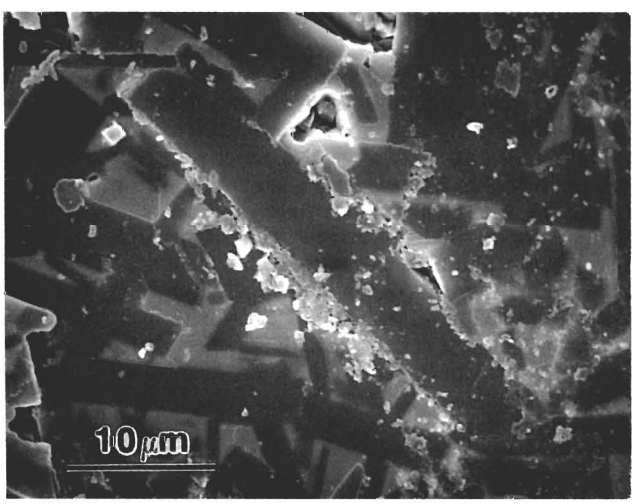

Fig. 4. Scanning electron micrographs of Hertzian cyclic-contact damage in heterogeneous silicon carbide from center regions of subsurface damage zones in Fig. 2(G). Note surface cavities from material removal and sliding-interface debris.

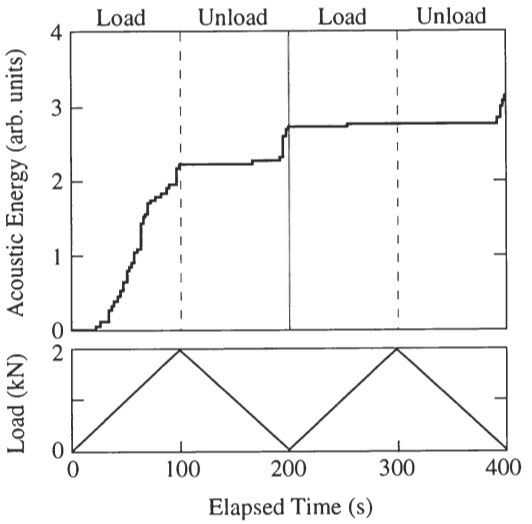

Fig. 5. Cumulative acoustic energy (arbitrary linear scale) versus elapsed time in heterogeneous silicon carbide. Data from initial load–unload–reload cycles (n = 1–2), tungsten carbide sphere of radius 3.18 mm, linear load ramps over 0–2000 N (lower diagram), tests in air.

Figure 5 is a plot for the first two cycles of one run over a minimum–maximum load range 0–2000 N. In the first half-cycle, acoustic activity begins after an initially passive period and then accelerates steadily up to the peak load. Virtually no emission is recorded during the first 80% of the unloading half-cycle, but then a burst of activity occurs in the final 20%. By contrast, in the second cycle virtually no emission is recorded during reloading, but a burst of activity again occurs in the final stage of unloading.

To investigate the fatigue activity further, data for nine reload–unload cycles (n = 2–10) in a second run over the same load range are plotted in Fig. 6. In this diagram we arbitrarily reset the time and cumulated energy origin to zero after completion of the first full cycle, to facilitate easy comparison with

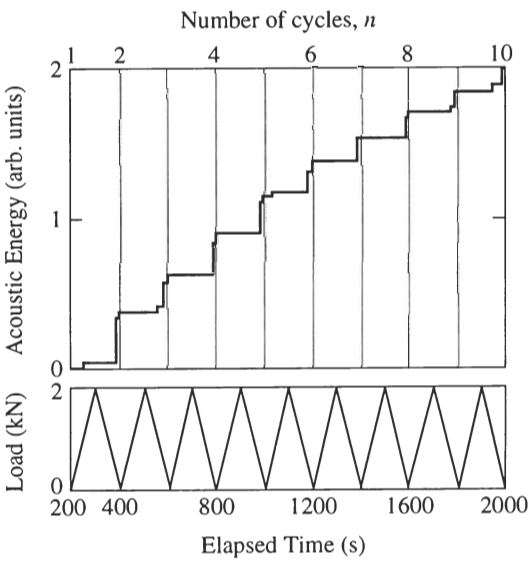

Fig. 6. Same as Fig. 5, again for linear load ramps over 0–2000 N but showing data from reload–unload cycles (n = 2–10). (In this diagram counting is arbitrarily started at completion of first load–unload cycle.)

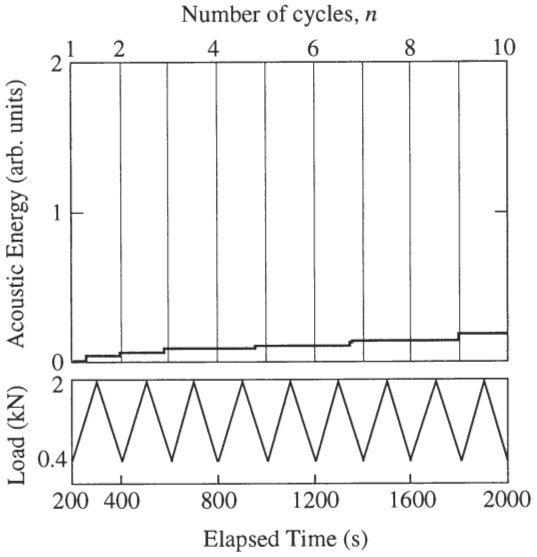

Fig. 7. Same as Fig. 6, but for linear reload–unload ramps over 400–2000 N.

Fig. 7 below. Bursts of activity continue to occur toward the end of each unload stage. Again, the implication of reversal in the frictional sliding process at the weak microstructural interfaces is manifest.

Figure 7 represents a similar run, but with minimum load 400 N in the reload–unload cycles. The cumulative acoustic emission is markedly reduced relative to that in Fig. 6, consistent with the reduced damage accumulation observed in the sequence of micrographs in Fig. 3 relative to Fig. 2. The truncation in the unloading cycle appears to have largely suppressed the reversal in the micromechanical sliding process.

(3) Strength

Figure 8 plots the strengths of indented silicon carbide specimens as a function of number of Hertzian cycles n over the contact load range 0–1000 N. Each point is the mean and standard deviation of a minimum five specimens for each material at each specified n. Boxes at the left axis represent base laboratory strengths, i.e., for specimens that failed from microstructural flaws.

For the homogeneous silicon carbide, the mean strength drops precipitously after a single cycle, from base value 452 MPa to 208 MPa, due to the invariable formation of a cone crack below the peak load 1000 N. Further degradation with subsequent cycling is initially slight, amounting to a decline to just under 200 MPa at $n = 10^5$, but is then followed by an accelerated decline to 172 MPa at $n = 10^6$. The initial slight decline may be attributed to the chemical influence of atmospheric moisture on cone-crack depth[28]—the solid curve in Fig. 8 is a prediction of such a chemical influence from literature crack velocity data for silicon carbide (Appendix). The accelerated decline toward the end of the cycling range may be associated with residual contact stresses from the fine-scale subsurface deformation apparent in Figs. 1(F) and 1(G)[29,30] or to some other spurious mechanical effect.

By contrast, the strength of the heterogeneous silicon carbide hardly degrades at all from the base value 353 MPa for unindented specimens over the first few thousand cycles. Beyond $n \approx 10^4$ the strength begins to fall off more rapidly, to 215 MPa at $n = 10^6$, toward the strength level for the homogeneous material. This accelerated falloff correlates directly with the marked intensification of subsurface damage and ultimate formation of deleterious radial cracks at the end of the micrograph sequence in Fig. 2. Thus, in this material the answer to the issue of strength degradation rests with the weak-interface attrition process alluded to in Sect. III(1).

The falloff in strength in the heterogeneous silicon carbide at large n values raises the issue of damage tolerance in this material. In this context, it needs to be emphasized that the operating contact load of 1000 N used in obtaining the data in Fig. 8 produces noticeable starting damage in the first cycle. At some lower load, the degree of starting damage, and thence the rate of ensuing degradation, might be substantially suppressed. To test this hypothesis, some supplementary strength tests were run on specimens indented at half the above peak load, i.e., at 500 N. The resulting strength 287 MPa at $n = 10^6$ was closer to the laboratory strength (353 MPa) than to the fully cycled strength at 1000 N load (215 MPa). Therefore, it appears that there is an upper limit in peak operating load below which the strength of the heterogeneous silicon carbide may be maintained over a given number of cycles.

IV. Discussion

We have demonstrated that microstructure is a crucial factor in the Hertzian contact fatigue of silicon carbide. Control tests on a homogeneous, low-toughness material reveal a classical cone fracture pattern, with only slight degradation by crack extension in cyclic loading (Fig. 1). Part of this slight degradation is attributable to chemical interaction with atmospheric moisture, which has continuous access to the loaded crack via the open mouth at the specimen surface. A secondary effect is also in evidence, as the detached collar in the near-surface region of the cone crack (Fig. 1(G)), suggesting some kind of dissipative mechanical process in this region. Analogous tests on the heterogeneous, enhanced-toughness material show an altogether different contact response, consisting of a distributed zone of damage which expands steadily in density and scale with cycling (Figs. 2 and 3). Since, under the loading conditions of our experiments, the damage zone after the first cycle is wholly contained subsurface (Fig. 2(A)), it is reasonably concluded that atmospheric chemistry is not a factor in the initial zone expansion; i.e., the primary fatigue process in the heterogeneous silicon carbide is essentially mechanical rather than chemical. Ultimately, the heterogeneous material degrades to the point that grains are on the verge of wholesale dislodgement from the indentation zone (Fig. 2(G)).

The scanning electron micrographs in Fig. 4 show distinctive evidence for the underlying nature of the mechanical degradation in the heterogeneous material, in the form of surface debris. Similar debris has been observed ahead of notches in compression fatigue tests in several ceramics[17,31,32] and at bridging sites in long-crack fatigue tests on alumina.[18,33] The indication of frictional attrition from forward–reverse sliding at shear-fault interfaces between the silicon carbide platelets and YAG second phase is compelling. The acoustic emission results (Figs. 5–7) indicate unload–reload hysteresis at these sliding interfaces during the cycling. A strong precedent for hysteretic forward–reverse interfacial sliding at internal faults under compression–shear loading exists in the rock mechanics literature.[34]

The residual strength after cyclic Hertzian contact at peak load 1000 N (Fig. 8) provides a quantitative measure of degradation. In the homogeneous material, the strength drops abruptly after a single cycle, as a result of the cone crack pop-in, but further falloff with cycling is slight. In the heterogeneous material, the strength loss is initially slight from the initiation of subsurface damage, but accelerates as the damage intensifies beyond $n > 10^4$. At lower contact loads, this accelerated degradation in the heterogeneous material is largely suppressed within the cycle range covered (Sect. III(3)). Hence, the damage tolerance of this material over a specified cyclic lifetime is highly contingent on the operating load.

These observations have implications in the design and mode of failure in ceramic components, especially in bearing applications. The normal load 1000 N (contact pressures 6 GPa) used in the bulk of our experiments is of the order of those achieved in actual bearings.[35,36] Of course, in bearing applications the contact stress fields are expected to be somewhat more complex

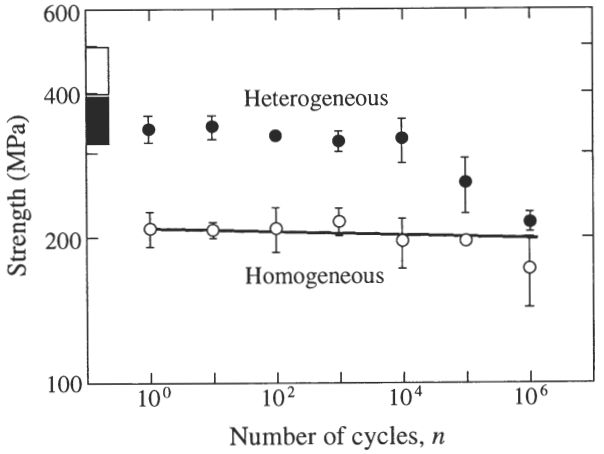

Fig. 8. Strength as a function of number of indentation fatigue cycles for homogeneous (open symbols) and heterogeneous (closed symbols) silicon carbide. Data points are means and standard deviations for 4–6 breaks. Curve through data for homogeneous material is predicted strength degradation from slow crack growth. Boxes at left axis represent failures from microstructural flaws. Note precipitous drop in strength in homogeneous material after $n = 1$, relatively slight drop in heterogeneous material. Cyclic fatigue tests in air, tungsten carbide sphere radius of 3.18 mm, sinusoidal load 0–1000 N at frequency 10 Hz.

than those in our idealized Hertzian configuration, involving rolling and perhaps sliding as well as normal loading. Nevertheless, the present tests serve to highlight the microstructural factors in the damage mode with minimum complexity. Thus, in the homogeneous silicon carbide we see little apparent fatigue tendency, but the potential for catastrophic failure from the cone crack system remains high. In the heterogeneous silicon carbide, the progression of cyclic damage appears more pronounced, but the damage is more benign, at least up to a million cycles (Fig. 8). On the other hand, the heterogeneous material is more susceptible to wear by microstructural attrition and dislodgement (Fig. 2(G)).[37,38] This tendency to enhanced material removal suggests the prospect of enhanced machinability in ceramics with contiguous weak interfaces.[39]

The observations presented in the present study provide the basis for constructing a micromechanical model of damage in ceramics with contiguous platelet structures.[40] The central element of the model is a platelet–matrix fault interface weak in shear. Above some critical shear stress in the subsurface contact field, the interface debonds and begins to slide. Compressive contact stresses maintain closure at the interface, so that sliding is resisted by Coulomb friction.[9,34,41,42] Removal of the confining compression (by unloading the indenter) allows the shear fault to reverse its sliding direction. In successive load–unload cycles, the friction diminishes by attrition, with consequent degradation of the microstructure and diminished compliance in the damage zone. As the damage zone becomes more compliant with successive cycles, the contact stress transfers to the surrounding material, enabling the damage to expand and densify further. Ultimately, adjacent faults interact and effectively coalesce, leading to material removal. There is no evidence in our observations for extensive associated microfracture in the damage zone in the heterogeneous silicon carbide; however, in other brittle ceramics extensile "wing" cracks may evolve at the edges of nonintersecting sliding faults to enhance the damage process.[9,41,42] The macroscopic stress–strain response of the material beneath the contact is the sum over all individual sliding elements within the damage zone through the cyclic evolution.

We conclude that microstructural heterogeneity, here in the form of contiguous elongate platelets with weak interphase boundaries, can have a profound effect on contact fatigue. Weak interfaces and long grains improve long-crack toughness and flaw tolerance, but also increase the susceptibility to damage accumulation in cyclic fatigue. Internal friction is another vital element in the damage susceptibility. Once micromechanical models of the damage process are developed, it should be possible to optimize microstructural characteristics to meet specific properties requirements for specific ceramic systems in repetitive loading.

APPENDIX

Effect of Slow Crack Growth on Strength Degradation from Extension of Cone Crack in Cyclic Contact

We compute the strength degradation of homogeneous silicon carbide due to slow cone crack growth from atmospheric moisture in Hertzian cyclic loading. For simplicity, assume a power-law velocity function

$$v = v_0(K/T_0)^N \tag{A-1}$$

where N is the velocity exponent and v_0 is a velocity coefficient, and T_0 is the single-valued toughness for this material.

The stress-intensity factor for the fully developed cone fracture (characteristic crack dimension $c >>$ contact radius) has the traditional form for pennylike cracks:[12]

$$K = \chi P/c^{3/2} \tag{A-2}$$

with P the contact load and χ a dimensionless geometry coefficient. Since the cone crack always pops in during the first half-cycle at the loads used in our homogeneous material, and since K is a diminishing function of c in Eq. (A-2), we may assume to first approximation that Eq. (A-2) holds from inception of the fatigue test.

For periodic load $P = P(t)$ with frequency f, we may compute the cone crack size after an integral number of cycles n. Combining Eqs. (A-1) and (A-2) gives

$$\int_0^c c^{3N/2}\,dc = v_0(\chi/T_0)^N \int_0^{n/f} [P(t)]^N\,dt \tag{A-3}$$

If we define the dimensionless quantity[24]

$$g(N) = f\int_0^{1/f} [P(t)/P^*]^N\,dt \tag{A-4}$$

we may integrate Eq. (A-3) to yield $c(n)$

$$c^{3N/2+1} = (nv_0/f)(\chi P^*/T_0)^N g(N) \tag{A-5}$$

The failure strength of specimens with cone cracks of dimension c subjected to n such contact cycles may be written in the familiar form[43]

$$\sigma_F = T_0/\Psi c^{1/2} \tag{A-6}$$

where Ψ is a crack geometry coefficient. Combining Eqs. (A-5) and (A-6), we may write the strength after n cycles relative to that after a single cycle in the normalized form

$$\sigma_F(n) = \sigma_F(1) n^{1/(3N+2)} \tag{A-7}$$

For homogeneous silicon carbide, setting the single-cycle strength at $\sigma_F(1) = 215$ MPa (Sect. III(3)) and the velocity exponent $N = 118$,[44] we evaluate the curve plotted in Fig. 8.

Acknowledgment: We thank H. H. K. Xu for experimental assistance.

References

[1]N. P. Padture, "*In Situ* Toughened Silicon Carbide," *J. Am. Ceram. Soc.*, **77** [2] 519–23 (1994).

[2]N. P. Padture and B. R. Lawn, "Toughness Properties of a Silicon Carbide with an *In Situ* Induced Heterogeneous Grain Structure," *J. Am. Ceram. Soc.*, in press.

[3]B. R. Lawn, N. P. Padture, H. Cai, and F. Guiberteau, "Making Ceramics 'Ductile,' " *Science (Washington, DC)*, **263**, 1114–16 (1994).

[4]Y.-W. Mai and B. R. Lawn, "Crack Stability and Toughness Characteristics in Brittle Materials," *Ann. Rev. Mater. Sci.*, **16**, 415–39 (1986).

[5]Y.-W. Mai and B. R. Lawn, "Crack-Interface Grain Bridging as a Fracture Resistance Mechanism in Ceramics: II, Theoretical Fracture Mechanics Model," *J. Am. Ceram. Soc.*, **70** [4] 289–94 (1987).

[6]S. J. Bennison and B. R. Lawn, "Flaw Tolerance in Ceramics with Rising Crack-Resistance Characteristics," *J. Mater. Sci.*, **24**, 3169–75 (1989).

[7]S. J. Bennison, N. P. Padture, J. L. Runyan, and B. R. Lawn, "Flaw-Insensitive Ceramics," *Philos. Mag. Lett.*, **64** [4] 191–95 (1991).

[8]F. Guiberteau, N. P. Padture, H. Cai, and B. R. Lawn, "Indentation Fatigue: A Simple Cyclic Hertzian Test for Measuring Damage Accumulation in Polycrystalline Ceramics," *Philos. Mag. A*, **68** [5] 1003–16 (1993).

[9]B. R. Lawn, N. P. Padture, F. Guiberteau, and H. Cai, "A Model for Microcrack Initiation and Propagation beneath Hertzian Contacts in Polycrystalline Ceramics," *Acta Metall.*, **42** [5] 1683–93 (1994).

[10]H. Cai, M. A. Stevens Kalceff, and B. R. Lawn, "Deformation and Fracture of Mica-Containing Glass–Ceramics in Hertzian Contacts," *J. Mater. Res.*, **9** [3] 762–70 (1994).

[11]H. H. K. Xu, L. Wei, N. P. Padture, B. R. Lawn, and R. L. Yeckley, "Effect of Microstructural Coarsening on Hertzian Contact Damage in Silicon Nitride," *J. Mater. Sci.*, **30**, 869–78 (1995).

[12]B. R. Lawn and T. R. Wilshaw, "Indentation Fracture: Principles and Applications," *J. Mater. Sci.*, **10** [6] 1049–81 (1975).

[13]M. V. Swain and B. R. Lawn, "A Study of Dislocation Arrays at Spherical Indentations in LiF as a Function of Indentation Stress and Strain," *Phys. Status Solidi*, **35** [2] 909–23 (1969).

[14]F. C. Roesler, "Brittle Fractures Near Equilibrium," *Proc. Phys. Soc., London*, **B69**, 981 (1956).

[15]F. C. Frank and B. R. Lawn, "On the Theory of Hertzian Facture," *Proc. R. Soc. London, A*, **299** [1458] 291–306 (1967).

[16]R. O. Ritchie, "Mechanisms of Fatigue Crack Propagation in Metals, Ceramics, Composites: Role of Crack-Tip Shielding," *Mater. Sci. Eng. A*, **103**, 15 (1988).

[17]S. Suresh, *Fatigue of Materials*. Cambridge University Press, Cambridge, U.K., 1991.

[18]S. Lathabai, J. Rödel, and B. R. Lawn, "Cyclic Fatigue from Frictional Degradation at Bridging Grains in Alumina," *J. Am. Ceram. Soc.*, **74** [6] 1340–48 (1991).

[19]R. H. Dauskardt, "A Frictional Wear Mechanism for Fatigue-Crack Growth in Grain Bridging Ceramics," *Acta Metall.*, **41** [9] 2765–81 (1993).

[20]H. Cai, M. A. S. Kalceff, B. M. Hooks, B. R. Lawn, and K. Chyung, "Cyclic Fatigue of a Mica-Containing Glass–Ceramic at Hertzian Contacts," *J. Mater. Res.*, **9** [10] 2654–61 (1994).

[21]F. Guiberteau, N. P. Padture, and B. R. Lawn, unpublished work.

[22]D. B. Marshall, "An Improved Biaxial Flexure Test for Ceramics," *Am. Ceram. Soc. Bull.*, **57** [5] 551–53 (1980).

[23]T. R. Wilshaw, "The Hertzian Fracture Test," *J. Phys. D: Appl. Phys.*, **4** [10] 1567–81 (1971).

[24]A. G. Evans and E. R. Fuller, "Crack Propagation in Ceramic Materials under Cyclic Loading Conditions," *Metall. Trans.*, **5** [1] 27–33 (1974).

[25]F. Guiberteau, N. P. Padture, and B. R. Lawn, "Effect of Grain Size on Hertzian Contact in Alumina," *J. Am. Ceram. Soc.*, **77** [7] 1825–31 (1994).

[26]J. A. Ryan, J. J. Grossman, and W. M. Hansen, "Adhesion of Silicates Cleaved in Ultrahigh Vacuum" *J. Geophys. Res.*, **73** [18] 6061–70 (1968).

[27]D. T. Smith and R. G. Horn, "Surface Forces and Adhesion between Dissimilar Materials Measured in Various Environments"; pp. 3–9 in *Tailored Interfaces in Composite Materials*, Vol. 170. Edited by C. G. Pantano and E. J. H. Chen. Materials Research Society, Pittsburgh, PA, 1990.

[28]M. V. Swain and B. R. Lawn, "A Microprobe Technique for Measuring Slow Crack Velocities in Brittle Solids," *Int. J. Fract. Mech.*, **9** [4] 481–83 (1973).

[29]D. B. Marshall and B. R. Lawn, "Residual Stress Effects in Sharp-Contact Cracking: I. Indentation Fracture Mechanics," *J. Mater. Sci.*, **14** [8] 2001–12 (1979).

[30]D. B. Marshall, B. R. Lawn, and P. Chantikul, "Residual Stress Effects in Sharp-Contact Cracking: II. Strength Degradation," *J. Mater. Sci.*, **14** [9] 2225–35 (1979).

[31]L. Ewart and S. Suresh, "Crack Propagation in Ceramics under Cyclic Loads," *J. Mater. Sci.*, **22**, 1173–92 (1987).

[32]S. Suresh and J. R. Brockenbrough, "Theory and Experiments of Fracture in Cyclic Fatigue Compression: Single Phase Ceramics, Transforming Ceramics and Ceramic Composites," *Acta Metall.*, **36** [6] 1455–70 (1988).

[33]R. H. Frei and G. Grathwohl, "Development of a Piezoelectric-Based Bending Device for In Situ SEM Investigations of High-Performance Ceramics," *J. Phys. E: Sci. Instrum.*, **22**, 589–93 (1989).

[34]J. C. Jaeger and N. G. W. Cook, *Fundamentals of Rock Mechanics*. Chapman and Hall, London, U.K., 1971.

[35]R. N. Katz and J. G. Hannoosh, "Ceramics for High Performance Rolling Element Bearings: A Review and Assessment," *Int. J. High Tech. Ceram.*, **1**, 69–79 (1985).

[36]J. W. Lucek, "Rolling Wear of Silicon Nitride Bearing Materials"; presented at Gas Turbine and Aeroengine Congress and Exposition (Brussels, Belgium, 1990), Paper No. 90-GT-165. American Society of Mechanical Engineers, New York, 1990.

[37]S.-J. Cho, B. J. Hockey, B. R. Lawn, and S. J. Bennison, "Grain-Size and *R*-Curve Effects in the Abrasive Wear of Alumina," *J. Am. Ceram. Soc.*, **72** [7] 1249–52 (1989).

[38]S.-J. Cho, H. Moon, B. J. Hockey, and S. M. Hsu, "The Transition from Mild to Severe Wear in Alumina during Sliding," *Acta Metall.*, **40** [1] 185–92 (1992).

[39]N. P. Padture, C. J. Evans, H. H. K. Xu, and B. R. Lawn, "Enhanced Machinability of a Silicon Carbide via Microstructural Design," *J. Am. Ceram. Soc.*, **78** [1] 215–17 (1995).

[40]N. P. Padture and B. R. Lawn, "Fatigue in Ceramics with Interconnecting Weak Interfaces: A Study Using Cyclic Hertzian Contacts," *Acta Metall.*, **43** [4] 1609–17 (1995).

[41]H. Horii and S. Nemat-Nasser, "Brittle Failure in Compression: Splitting, Faulting and Brittle–Ductile Transition," *Philos. Trans. R. Soc. London*, **319** [1549] 337–74 (1986).

[42]M. F. Ashby and S. D. Hallam, "The Failure of Brittle Solids Containing Small Cracks under Compressive Stress States," *Acta Metall.*, **34** [3] 497–510 (1986).

[43]B. R. Lawn, *Fracture of Brittle Solids*, 2nd ed. Cambridge University Press, Cambridge, U.K., 1993.

[44]K. D. McHenry, T. Yonushonis, and R. E. Tressler, "Low-Temperature Subcritical Crack Growth in SiC and Si_3N_4," *J. Am. Ceram. Soc.*, **59** [5–6] 262–63 (1976). □